05627-5-S

THE UNIVERSITY OF MICHIGAN

COLLEGE OF ENGINEERING
DEPARTMENT OF AEROSPACE ENGINEERING
HIGH ALTITUDE ENGINEERING LABORATORY

Scientific Report

Surface Current Excitation on an Inhomogeneously-Sheathed Plasma Immersed Cylinder by Electromagnetic and Electrokinetic Waves

EDMUND K. MILLER

Under contract with:

National Aeronautics and Space Administration
Contract No. NASr-54(05)
Washington, D. C.

Administered through:

December 1966

OFFICE OF RESEARCH ADMINISTRATION • ANN ARBOR

THE UNIVERSITY OF MICHIGAN

COLLEGE OF ENGINEERING

Department of Aerospace Engineering

High Altitude Engineering Laboratory

Scientific Report

SURFACE CURRENT EXCITATION ON AN INHOMOGENEOUSLY-SHEATHED PLASMA IMMERSED CYLINDER BY ELECTROMAGNETIC AND ELECTROKINETIC WAVES

Edmund K. Miller

ORA Project 05627

Under contract with:

NATIONAL AERONAUTICS AND SPACE ADMINISTRATION

CONTRACT NO. NASr-54(05)

WASHINGTON, D. C.

administered through:

OFFICE OF RESEARCH ADMINISTRATION ANN ARBOR

December 1966

TABLE OF CONTENTS

LIST OF FIGURES

ABSTRACT

A theoretical investigation is described which analyzes the effect of an inhomogeneous sheath on the surface currents excited on an infinitely long, perfectly conducting, circular cylinder immersed in an isotropic collisionless, compressible plasma by plane electromagnetic (EM) and electrokinetic (EK) waves incident at an arbitrary angle with respect to the cylinder axis. The linearized fluid equations are used in the analysis, with the inhomogeneous sheath taken to extend a finite distance into the plasma from the cylinder surface, on the order of 10 electron Debye lengths, beyond which the plasma is uniform. The numerical results for the surface currents obtained from the inhomogeneous sheath analysis are compared with those obtained when the sheath is replaced by a free-space region, called the vacuum sheath. It is found that for EM wave incidence, the surface currents are practically independent of the sheath and the finite plasma temperature. For EK wave incidence, the sheath has an attenuating effect on the currents produced, compared with the sheathless case, with the attenuating effect of the vacuum sheath being greater than that of the inhomogeneous sheath.

1. Introduction

The effect of a finite plasma temperature (warm plasma, as opposed to the zero temperature or cold plasma) on the propagation of electromagnetic (EM) waves in a plasma medium is a subject which is of current interest. In the case of the cold plasma the effect of the plasma on the EM wave may be wholly accounted for by a suitable permittivity which is a function of the plasma parameters. The warm plasma can however, support in addition to the EM wave, an electron pressure wave, or the electrokinetic (EK) wave. This EK wave may couple to the EM wave in regions of plasma inhomogeneity and at bounding surfaces of the plasma, so that the plasma permittivity for the EM wave is by itself no longer sufficient to determine the effect of the plasma on EM waves propagating in it. The EM and EK waves may also be coupled by external magnetic fields and non-linear effects. The coupling mechanisms to be considered in this paper will be those due to gradients in the static electron number density (inhomogeneity coupling), and to plasma boundaries (boundary coupling).

The specific problem to be considered is an investigation of the surface currents which are excited on an infinitely long, circular, perfectly conducting cylinder by plane EM and EK waves. There are two reasons for this interest in the surface currents. (1) It is of value to determine whether it may be feasible to detect the presence of the EK wave in the plasma by a measurement of the surface current it may excite on the cylinder. Since the EK wave itself has no magnetic field, it can only excite a surface current as a result of coupling to the EM wave. (2) Also of interest is the effect of coupling to the EK wave on the currents excited by the EM wave. The EK wave can, for example lead to coupling between

the transverse-electric (TE) and transverse-magnetic (TM) polarizations of the EM wave scattered from a cylinder in a warm plasma, whereas such coupling does not occur in the cold plasma. The relative influence of inhomogeneity coupling and boundary coupling on the currents due to both the EK and EM wave will be examined, as well as the effects of the various plasma parameters.

The linearized hydrodynamic equations will be used to account for the medium behavior of the plasma, together with Maxwell's equations. While the frequency range over which the hydrodynamic approach is reliable is confined to a rather narrow interval about the electron plasma frequency, it is sufficient for the present problem. We are concerned in the analysis with frequencies (f) above the plasma frequency (f_P) and below the frequency where Landau damping becomes important, roughly $\sqrt{2}\, f_P$, since the hydrodynamic approach does not account for Landau damping. The numerical results will be presented for $N=f_P/f=0.7$ only because of the time consuming nature of the calculations.

2. Formulation of the Problem

We take the infinitely long, perfectly conducting, circular cylinder to be oriented with its axis coincident with the z-axis of the cylindrical coordinate system (ρ , φ , z). The cylinder is allowed to acquire its floating potential in the plasma, i.e., its potential is determined by the plasma parameters such as electron temperature and ion mass, so that the net current flowing to it is zero. As a result, the cylinder has a negative potential with respect to the plasma, and an inhomogeneous sheath forms about it in which there is a defeciency of electrons. This inhomogeneous sheath

extends out into the plasma, for practical purposes, up to 20 electron Debye lengths (D_ℓ) from the cylinder surface, beyond which charge neutrality is nearly restored. Consequently, as shown in Fig. 1, the plasma is divided into 2 regions. In the outer region, $\rho > s$, the plasma is taken to be spatially uniform, while the region between the sheath-uniform plasma interface (sheath interface) and cylinder surface, $c < \rho < s$, comprises the inhomogeneous sheath, which is thus taken to be of finite thickness. Because of the axial and azimuthal symmetry, the static sheath variables are functions of the radius ρ only. We will, for purposes of comparison, present some results for the case where the sheath region is replaced by a free-space layer, which separates the cylinder from the uniform plasma. This will be called the vacuum sheath model, and the situation where the sheath is of zero thickness will be called the sheathless case.

The equations from which the time-varying or dynamic field quantities in the plasma will be obtained are the usual linearized hydrodynamic and Maxwell's equations. These equations, after separation of variables and with an $e^{i\omega t}$ time dependence, lead to the following set of first order, ordinary differential equations (Miller and Olte, 1966b).

[1a] $$Q_n' = i\omega\epsilon E_n^{(\rho)} + i\frac{n}{\rho} H_n^{(z)} + i\beta H_n^{(\varphi)} - L_o Q_n$$

[1b] $$H_n^{(\varphi)'} = i\omega\epsilon E_n^{(z)} - \frac{1}{\rho} H_n^{(\varphi)} - i\frac{n}{\rho} H_n^{(\rho)} - i\beta Q_n$$

[1c] $$H_n^{(z)'} = -i\omega\epsilon E_n^{(\varphi)} + i\beta H_n^{(\rho)} - i\frac{n}{\rho} Q_n$$

[1d] $$E_n^{(\rho)'} = -\frac{1}{\rho} E_n^{(\rho)} + i\frac{n}{\rho} E_n^{(\varphi)} - i\beta E_n^{(z)} + \frac{i\omega}{\epsilon_o v_r^2} Q_n$$

[1e] $$E_n^{(\varphi)'} = -\frac{1}{\rho} E_n^{(\varphi)} - i\frac{n}{\rho} E_n^{(\rho)} - i\omega\mu_o H_n^{(z)}$$

[1f] $$E_n^{(z)'} = i\beta E_n^{(\rho)} + i\omega\mu_o H_n^{(\varphi)}$$

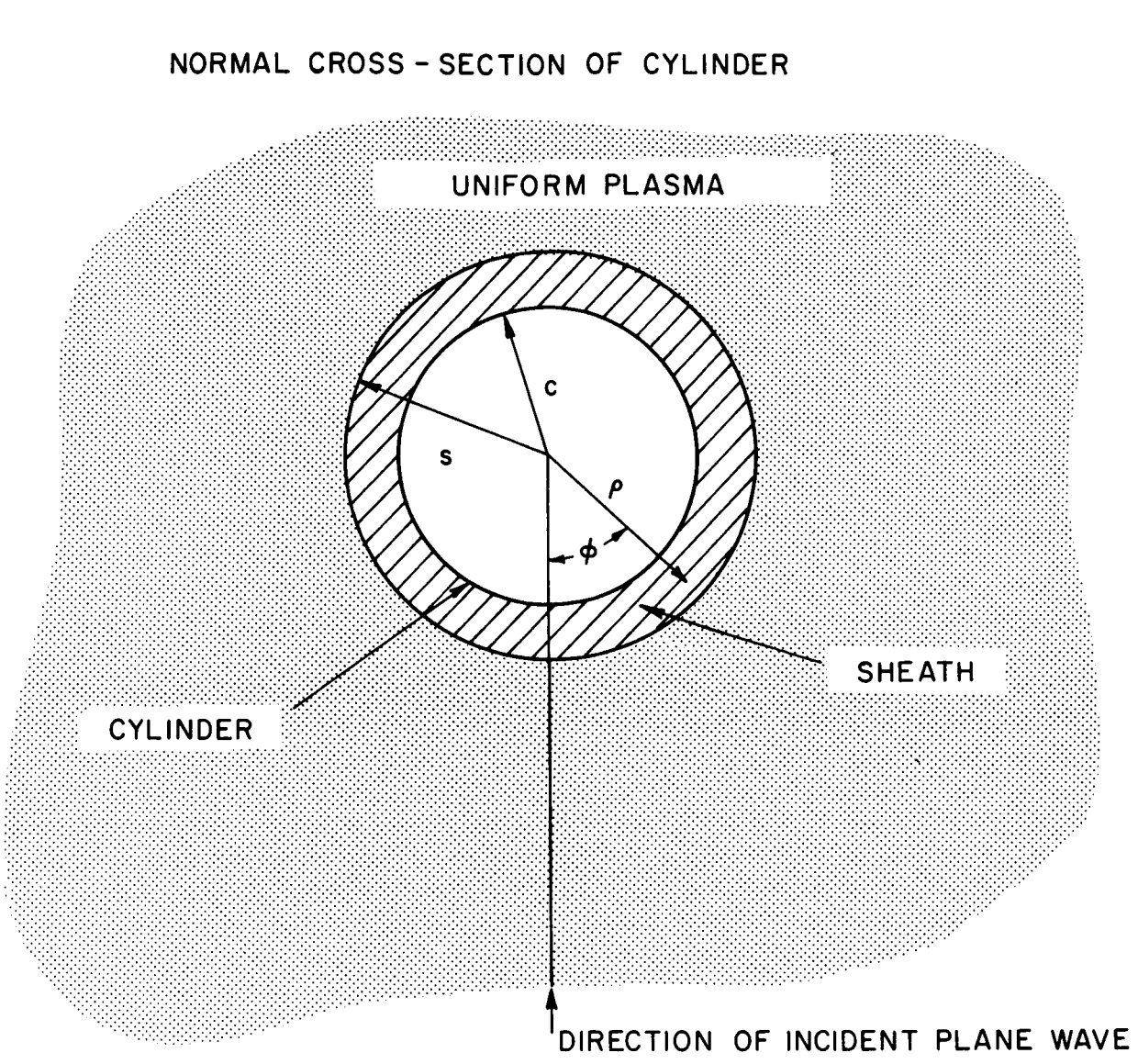

Fig. 1: Normal cross-section of the cylinder.

with

$$\omega_P^2 = e^2 n_o / \epsilon_o m = (2\pi f_P)^2$$

$$\epsilon_r = 1 - \omega_P^2 / \omega^2 = 1 - N^2$$

$$\epsilon = \epsilon_o \epsilon_r$$

$$L_o = e E_o / m v_r^2$$

$H_n^{(\rho)}$ is given by

$$[1g] \qquad H_n^{(\rho)} = \frac{n}{\omega \mu_o \rho} E_n^{(z)} + \frac{\beta}{\omega \mu_o} E_n^{(\varphi)}$$

while

$$[1h] \qquad \vec{V}_n = \frac{1}{e n_o} [-\nabla \times \vec{H}_n + i\omega \epsilon_o \vec{E}_n]$$

The subscript n, an integer, is the azimuthal separation constant, β is the z separation constant, the prime denotes differentiation with respect to the radial variable, and the superscript denotes the field component. The time varying electric and magnetic fields and electron velocity are represented by E, H, and V respectively, the static electric field and electron number density are given by E_o and n_o, and Q is related to the time varying electron number density n_1 by

$$[1i] \qquad Q = \frac{-e}{i\omega} v_r^2 n_1$$

Finally, -e and m are the electron charge and mass, v_r is the rms electron velocity, and ϵ_o and μ_o are the permittivity and permeability of free space. We may note that a closed form solution to the system of equations [1] is in general not possible for $E_o \neq 0$, i.e., in the sheath. Analytic solutions exist of course for the uniform plasma.

In order to complete this set of equations, we require a description for the static sheath from which n_o and E_o are found, as well as the fields of the incident plane wave and the boundary conditions to be applied. We obtain E_o and n_o as follows:

$$[2a] \qquad E_o = - \nabla \Phi_o$$

$$[2b] \qquad \Phi_o = \Phi_c \left[\frac{s-\rho}{s-c}\right]^M$$

$$[2c] \qquad \Phi_c = \frac{-kT}{e} \log\left[\sqrt{\frac{m_i}{m}}\ \frac{1}{1.22}\right]$$

$$[2d] \qquad n_o = n_{oo} \exp\left[\frac{e\Phi_o}{kT}\right]$$

with Φ_c the cylinder potential from an expression due to Self (1963), M a parameter which will have a value of 2 for the numerical results to be presented, k Boltzmann's constant, T the electron temperature, m_i the ion mass and n_{oo} the static electron density in the uniform plasma. A discussion of the applicability of using [2] to describe the static sheath is given by Miller (1966) and so will not be pursued here.

The fields of the incident and scattered waves in the uniform plasma can be obtained from potentials (Hansens' method) involving Fourier series of cylindrical Bessel functions and Hankel functions of the second kind respectively. We decompose the incident and scattered EM waves into the transverse electric (TE), $E^{(z)} = 0$, and transverse magnetic (TM), $H^{(z)} = 0$, polarizations, and use the subscripts e, m and p to differentiate quantities associated with the TE, TM and EK waves respectively. In the results to follow, the incident plane waves will have unit potential amplitude. The boundary conditions required to be satisfied at the sheath interface are continuity of the tangential electric field, the tangential magnetic field, the normal electron velocity and the time varying electron density. At the

cylinder surface, the tangential electric field is required to be zero due to the infinite conductivity of the cylinder. These requirements produce 8 scalar boundary condition equations, while 9 such equations are necessary, since in addition to the 6th order differential equation [1], the scattering coefficients of the TE, TM and EK waves in the uniform plasma are required. The one remaining boundary condition to be used will be an admittance relation between the normal electron velocity and time varying electron number density at the cylinder surface, of the kind introduced by Cohen (1962). These boundary conditions may be expressed in separated form as, at $\rho = s$:

$$[3a] \qquad \underset{\sim}{\rho} \times \left[(\underset{\sim}{E}_n)_{\text{plasma}} - (\underset{\sim}{E}_n)_{\text{sheath}} \right] = 0$$

$$[3b] \qquad \underset{\sim}{\rho} \times \left[(\underset{\sim}{H}_n)_{\text{plasma}} - (\underset{\sim}{H}_n)_{\text{sheath}} \right] = 0$$

$$[3c] \qquad \underset{\sim}{\rho} \cdot \left[(\underset{\sim}{V}_n)_{\text{plasma}} - (\underset{\sim}{V}_n)_{\text{sheath}} \right] = 0$$

$$[3d] \qquad (Q_n)_{\text{plasma}} - (Q_n)_{\text{sheath}} = 0$$

and at $\rho = c$:

$$[4a] \qquad \underset{\sim}{\rho} \times (\underset{\sim}{E}_n)_{\text{sheath}} = 0$$

$$[4b] \qquad \underset{\sim}{\rho} \cdot (\underset{\sim}{V}_n)_{\text{sheath}} = Y_B (Q_n)_{\text{sheath}}$$

where Y_B is the surface admittance. In solving [1], we eliminate the Fourier scattering coefficients of the fields in the uniform plasma, and so reduce the number of scalar boundary condition equations above from 9 to 6 equations involving the 6 field quantities whose derivatives appear in [1]. It may be observed in [4b] that for zero surface admittance ($Y_B = 0$), the electrons are elastically scattered from the cylinder surface, a situation described in acoustics as a hard boundary. If on the other hand, the surface admittance is infinite, then all the incident electrons are absorbed, a situation which is referred to as a soft boundary. Since there is no coupling

between the EM and EK waves at a soft boundary (Miller and Olte, 1966a), the latter case is of interest since then the surface currents excited by the EK wave will be due to inhomogeneity coupling alone. The hard boundary however leads to surface currents excited by the EK wave due to both inhomogeneity and boundary coupling. Consequently, a comparison of results for both the hard and soft boundaries allows us to obtain an idea of the relative importance of the inhomogeneity and boundary coupling mechanisms between the EK and EM fields.

This set of boundary condition equations together with the differential equations [1] constitute the problem to be solved. Note that the surface currents, the quantities of primary interest, are obtained from the tangential magnetic field at the cylinder surface. In the next section we discuss briefly the method of solution.

3. Method of Solution

a. General Discussion

The set of ordinary first order differential equations [1] together with the scalar boundary conditions [3] and [4] applied at the cylinder surface and sheath interface constitutes a two-point boundary value problem, as opposed to the initial value problem where the boundary condition equations are applied at a single value of the independent variable. While the initial value problem may be handled in a relatively straightforward way numerically, the boundary value problem is considerably more involved. This is because in the initial value problem the information required to calculate the starting values of all the dependent variables is given at a single point. Consequently, the differential equations can be used to evaluate the derivatives there and the integration is started by a standard technique

such as Runge-Kutta, for example, and the unique solution which satisfies the boundary conditions is obtained. In the boundary value problem however, there are fewer boundary condition equations than dependent variables at any one boundary. As a result, no matter at which boundary the integration is begun, there is insufficient information to determine the starting values of all the dependent variables at that boundary. This missing information is contained in the boundary condition equations at the second boundary, which cannot be utilized however until the integration has been carried out to the second boundary.

This difficulty is overcome in a straightforward way, at the expense of a considerable increase in computer time compared with the initial value problem. The procedure followed is to divide the dependent variables into two sets. The variables in the first set, equal in number to the number of boundary condition equations at the boundary A where the integration is started, are the "known" variables, whose starting values are determined from the boundary condition equations. The variables in the second set are the "unknown" variables, and are assigned arbitrary starting values in order to begin the integration. Denote the known variables by y_i, $i = 1, \ldots, J$ and the unknown variables by x_i, $i = 1, \ldots, I$ where $J + I$ is the total number of dependent variables. The set of differential equations [1] then constitute a transformation relating the derivatives f_i, $i = 1, \ldots, I + J$ of the dependent variables to the dependent variables themselves, as

$$[5] \qquad f_i(\rho) = \sum_{j=i}^{I+J} T_{ij}(\rho)\, z_j(\rho)$$

where $T_{ij}(\rho)$ is determined explicit ly by the differential equation and

$$z_i(\rho) = x_i(\rho) \; ; \; i = 1, \ldots, I$$

$$y_{i-I}(\rho) \; ; \; i = I + 1, \ldots, I + J$$

The boundary condition equations at the starting boundary A may be written

$$[6a] \qquad S_i(A) = \sum_{j=i}^{J+I} A_{ij} z_i(A) \; ; \; i = 1, \ldots, J$$

where $S_i(A)$ is the contribution of the source, if any, (in our case, the incident wave) at boundary A. Similarly at the boundary B where the integration is terminated

$$[6b] \qquad S_i(B) = \sum_{j=i}^{J+I} B_{ij} z_j(B) \; ; \; i = 1, \ldots, I$$

where the total number of scalar boundary condition is thus equal to the number of first order differential equation to be solved. Thus [6a] provides a relationship from which the J known variables $y_i(A)$ can be found in terms of the I unknown variables $x_i(A)$ at the starting boundary A.

We also observe that the starting values of all the derivatives $f_i(A)$ at boundary A may be written in terms of the $x_i(A)$. From [6a] we get

$$[7a] \qquad y_i(A) = \sum_{j=1}^{J} \overline{a}_{ij} \left(S_j(A) - \sum_{k=1}^{I} \tilde{A}_{jk} x_k(A) \right) \; ; \; i=1, \ldots, J$$

where

$$a_{ij} = A_{i, j+I} \qquad i, j = 1, \ldots, J$$

$$\overline{a}_{ij} = (a)^{-1}_{ij}$$

and $\tilde{A}_{ij}$ is the JxI submatrix of A_{ij} which remains after removing a_{ij}

$$\tilde{A}_{ij} = A_{ij} \qquad i = 1, \ldots, J$$

$$j = 1, \ldots, I$$

Then using [5] and [7a] we obtain

$$[7b] \qquad f_i(A) = \sum_{j=1}^{I} T'_{ij}(A) \, x_j(A) + S'_i(A); \; i=1, \ldots, I+J$$

with

$$T'_{ij}(A) = \tilde{\tilde{T}}_{ij}(A) - \sum_{k=1}^{J} \sum_{l=1}^{J} t_{ik}(A) \, \overline{a}_{kl} \, \tilde{\tilde{A}}_{lj}$$

$$S'_i(A) = \sum_{k=1}^{J} \sum_{j=1}^{J} t_{ij}(A) \, \overline{a}_{jk} \, S_k(A)$$

where $t_{ij} = T_{i,\ j+I}$ $\quad i = 1, \ldots, I + J$

$\quad j = 1, \ldots, J$

$\tilde{T}_{ij} = T_{ij}$ $\quad i = 1, \ldots, I + J$

$\quad j = 1, \ldots, I$

We note that in obtaining the starting values of the derivatives $f_i(A)$ from [7b] , the boundary condition equations [6a] are satisfied regardless of the values assigned to the $x_i(A)$. The problem now is to find the correct starting values for the $x_i(A)$ which lead to the unique solution that will satisfy [6b] as well as [6a]. The correct starting values $x_i(A)$ which result in satisfying both [6a] and [6b] are obtained as follows:

First choose a set of values $X_{ij}(A)$ for x_i at A, with j = 1, denoting this to be the first set of x_i to be so specified. It follows that [7b] can be written for the starting values $F_{ij}(A)$ in the form

$$F_{ij}(A) = \sum_{k=1}^{I} T'_{ik} X_{kj}(A); \quad \begin{matrix} i=1, \ \ldots, \ I + J \\ j=1 \end{matrix}$$
$$+ S'_i(A)$$

The integration can now be carried out to boundary B where the values $Z_{i1}(B)$ and $F_{i1}(B)$ are obtained. Unless our choice for $X_{i1}(A)$ has been extremely fortuitous, however, [6b] will not be satisfied by the value of $Z_{i1}(B)$ which results.

If we now repeat this process with other sets of values $X_{ij}(A)$, j=2 ..., I and form the linear combination

$$z_i(B) = \sum_{j=1}^{I} c_j Z_{ij}(B) \ ; \ i=1, \ \ldots, \ I + J$$

then [6b] provides the I equations from which the c_j can be found. Thus

[8a] $$c_j = \sum_{i=1}^{I} \overline{M}_{ji} \ S_j(B); \ j=1 \ \ldots, \ I$$

where

[8b] $$M_{ji} = \sum_{k=1}^{I+J} B_{jk} X_{ki}(B)$$

and $$\overline{M}_{ji} = (M)^{-1}_{ji}$$

The correct starting values of x_i at boundary A are then given by

[9] $$x_i(A) = \sum_{j=1}^{I} c_j X_{ij}(A)$$

and the unique solution to the problem may be obtained by a final integration using [7b] but now with $S_i'(A) \longrightarrow S_i'(A) \sum c_j$, or a combination of the previously calculated values $Z_{ij}(\rho)$

[10] $$z_i(\rho) = \sum_{j=1}^{I} c_j Z_{ij}(\rho)$$

In most problems of interest, such as scattering by an obstacle or the radiation from a source, one of the source vectors $S_i(A)$ or $S_i(B)$ will be zero. It may be convenient to integrate in the direction which makes $S_i(B)=0$. In that case [8] will not be applicable. If, however, one integration is performed with the $X_{ij}(A)=0$, which as shown by [7b] is not a trivial case, since $S_i(A)$ is then non zero and we denote this integration with j=o, then

[11] $$c_j = \sum_{i=1}^{I} \overline{M}_{ji} S_i'(B)$$

where $$S_i'(B) = - \sum_{j=1}^{I+J} B_{ij} Z_{jo}(B)$$

The c_j are then found in terms of $Z_{jo}(B)$. Since $Z_{jo}(B)$ is proportional to the source strength $S_i(A)$ at A, we see that the c_j obtained are proportional to $S_i(A)$, in a similar fashion to [8] where the c_j are proportional to $S_i(B)$.

The j sets of starting values $X_{ij}(A)$ may be chosen arbitrarily with the restriction that

$$\sum_{j=1}^{I} \alpha_j X_{ij}(A) = 0$$

have only the trivial solution $\alpha_j \equiv 0$. This requirement that the $X_{ij}(A)$ be linearly independent follows from [8b] that the matrix M_{ij} have are inverse.

A disadvantage of the numerical solution of the boundary value problem compared with the initial value problem is thus seen to be the necessity for performing the numerical integration of the J + I differential equation a total of I + 1 times. (I times are required to evaluate c_j and the last time is required for the final answer.) The computation time is thus made at least I + 1 times as great for the former problem. Consequently, it is advantageous to begin the integration at the boundary where I has the smaller value.

It is also apparent for a given integration step-size, that the results obtained for the boundary value problem cannot be expected to be as accurate as those obtained for the initial value problem. This is due to the fact that the accuracy of the starting values $x_i(A)$ is dependent upon the precision with which the I integration can be performed and the matrix [8b] inverted. While each individual integration can be performed with the same relative accuracy, the errors accumulate in the matrix inversion and this can in some cases lead to errors in the c_j coefficients of much larger magnitude than those arising from the integration.

b. Application to the Problem Under Consideration

If the scattering coefficients for the fields in the uniform plasma are eliminated in the boundary condition equation [3], the sheath field quantities $E_n^{(\rho)}$, $E_n^{(\varphi)}$, $E_n^{(z)}$, Q_n, $H_n^{(\varphi)}$, and $H_n^{(z)}$ are the only dependent variables appearing in them. There will then be three boundary condition equations at each boundary, so that I = J = 3 regardless at which boundary the integration begins. Thus the variables $E_n^{(\rho)}$, $E_n^{(\varphi)}$, and $E_n^{(z)}$, were used as the set of known variables, while Q_n, $H_n^{(\varphi)}$ and $H_n^{(z)}$ were the unknown variables.

A 4th order Runge-Kutta method was used to obtain the first three points in the solution. Then a 4th order predictor-corrector method due to Hamming (see Ralston, 1965, p. 189) was utilized, to continue the integration. At each integration point, an estimate of the error bound associated with each variable was obtained as discussed by Ralston (1965, p. 203). If the error bound associated with any variable was found to be larger than the desired minimum accuracy, there were two options which could be followed. The predictor-corrector routine could be iterated, as many times as necessary to decrease the error-bound below the desired level, assuming the iterated values converged, or the integration step-size could be decreased. It was found that if one iteration of the predictor-corrector routine was insufficient to produce the desired decrease in the error, it was more efficient to halve the integration step-size. This involves again using the Runge-Kutta method to set up the required values of the variables for the predictor-corrector routine for the new step size. If on the other hand, all of the error bounds were smaller than the maximum desired accuracy, then for reasons of economy, the step-size was doubled. Otherwise, the integration step-size was left unchanged.

The integration routine was programmed so that the integration could be started at either the sheath interface or cylinder surface. Some calculations were carried out with the cylinder potential $\Phi_c = 0$, i.e. the sheathless case, in order to compare the accuracy of the numerical integration with the analytic solutions that can be obtained in this case (Miller and Olte, 1966a). It was found that the numerical integration produced results for the surface current in agreement with the analytic solution to 3 or 4 significant figures when the integration was begun at the sheath interface, for an EK

wave at an angle of incidence $\theta^i = 9^o$ measured from the positive z axis. This accuracy could be obtained for sheath thicknesses on the order of $10D_\ell$ or less, so that the results to be presented are restricted to sheaths no thicker than $10D_\ell$.

When the integration was begun at the cylinder surface however, the numerical integration results for the surface current were generally unreliable. This occurs since the EM fields, for this angle of EK wave incidence, are evanescent, decaying exponentially with increasing radius, and the integration, in order to accurate, should proceed in the direction of increasing field magnitude. For EM wave incidence, and for EK wave incidence at an angle such that radially propagating EM fields are produced, the integration could be begun at either the sheath interface a cylinder surface with 3 to 4 figure agreement with the analytic solution.

The most obvious set of starting values $X_{ij}(A)$ is the identity matrix. However, it was found in practice that the error-bounds associated with the variables with a starting value of zero were generally larger than that of the variable with the starting value of unity. This may indicate that it is not physically realistic for example, to have both Q_n and $H_n^{(\varphi)}$ equal to 0 at the starting boundary. Thus the matrix of starting values $X_{ij}(A)$ used had 2's on the diagonal and 1's elsewhere. The matrix M_{ij} was inverted in double precision (16 places) to obtain the c_j. The final values for the field variation in the sheath was obtained from [10], i.e., by storing the results of each separate integration. This was done, rather than performing the integration a final time, since the values for c_j are less accurately known than the $Z_{ij}(\rho)$, so that the errors in the final $z_i(\rho)$ are kept on the order of the errors in the c_j rather than becoming further increased as a result of the

final integration. This also shortens the computation time by eliminating the final integration step.

4. Numerical Results

a. Incident EK Wave

In figs. 2 and 3 are shown the magnitudes of the φ and z components of surface current excited by the EK wave, $K_p^{(\varphi)}$ and $K_p^{(z)}$, for an angle of incidence θ^i of 9^o and a sheath thickness X, of 5 D_ℓ. There are two curves on the graphs, one each for the soft and the hard boundary. The vertical scale is amperes/cm and the horizontal scale, showing the azimuthal angle φ, runs from 0^o to 180^o only, since the currents are symmetric in φ. The cylinder potential is -5.34 volts, corresponding to a mercury plasma (m_i=200 atomic mass units) for electrons at a temperature of 10^4 ^oK, and the parameter M for the static potential, has a value of 2. The incident wave frequency f is 1 Gc/s and the plasma frequency f_P is 0.7 Gc/s ($N = f_P/f = 0.7$). For purposes of comparison, Figs. 4 and 5 show $K_p^{(\varphi)}$, and $K_p^{(z)}$ obtained from the vacuum sheath analysis for the same parameter values as figures 2 and 3 for various vacuum sheath thicknesses.

It may be seen in Figs. 2 and 3 that the current magnitude of $K_p^{(z)}$ for the hard boundary is similar to that for the soft boundary but roughly a factor of two larger, while $K_p^{(\varphi)}$ shows more variation between the hard and soft boundaries in the behavior as a function of φ. As a matter of fact, $K_p^{(\varphi)}$ for the soft boundary exceeds that for the hard boundary near the back of the cylinder. We might conclude from these curves that the contribution to the surface current excited by the EK wave due to the boundary and inhomogeneity coupling are of nearly the same magnitude. It should be noted in this regard, that the spatial distribution of n_1 is the sheath is dependent upon the

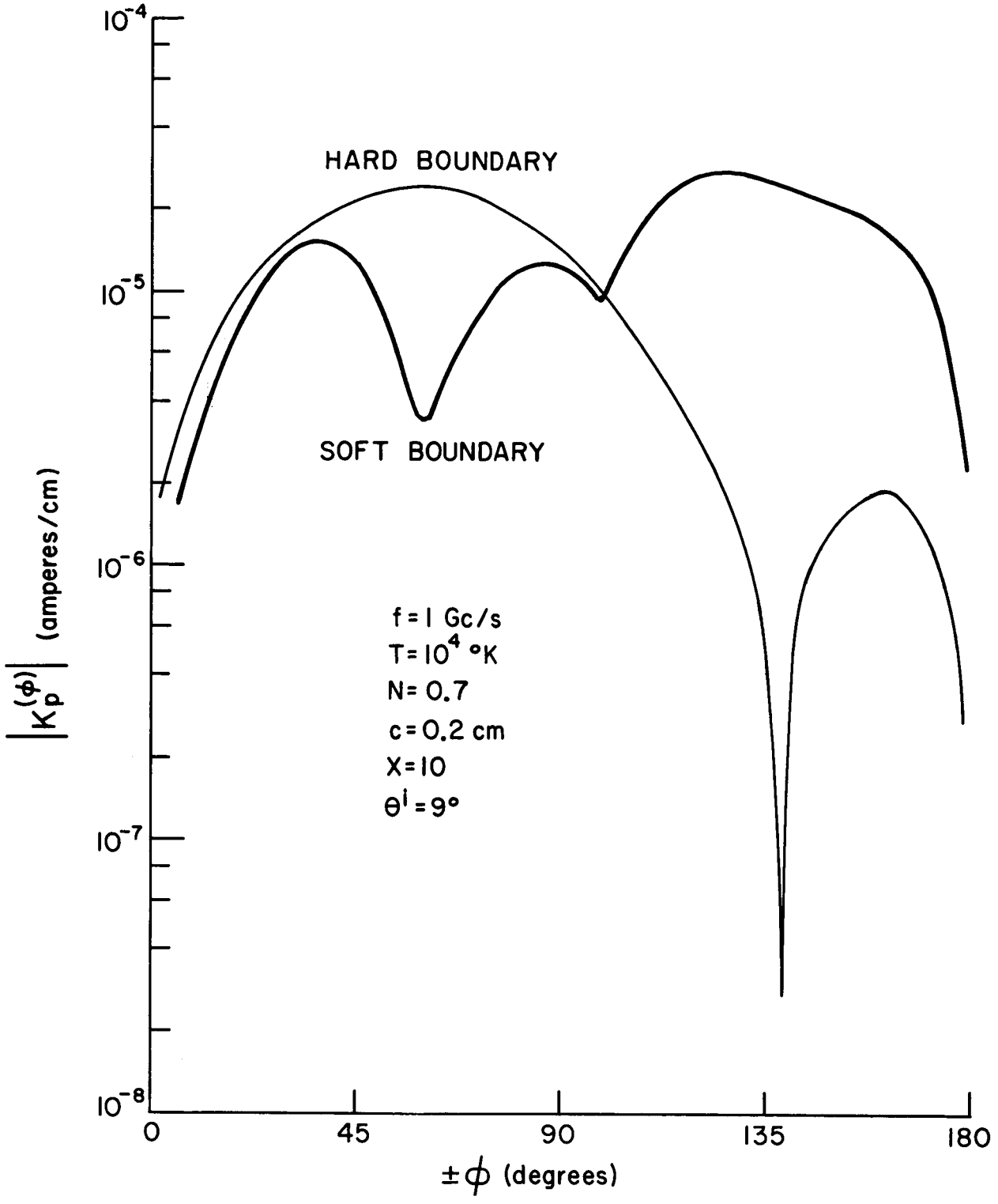

Fig. 2: The magnitude of $K_p^{(\varphi)}$ as a function of azimuthal angle φ for the inhomogeneous sheath model, with X = 5 and $\theta^i = 9^o$.

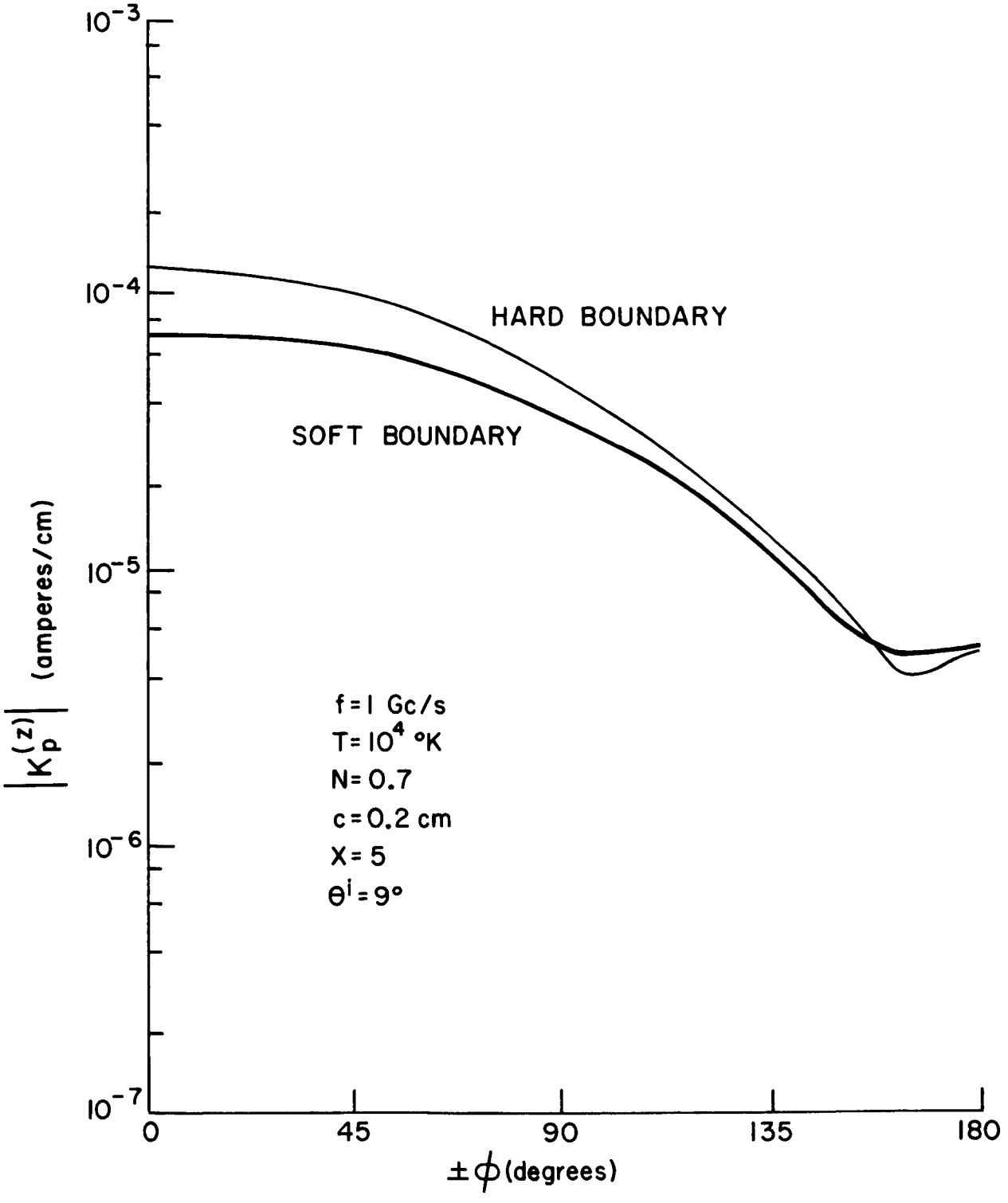

Fig. 3: The magnitude of $K_p^{(z)}$ as a function of azimuthal angle φ for the inhomogeneous sheath model, with X = 5 and $\theta^i = 9^o$.

value of Y_B. Consequently, the contributions of both the inhomogeneity coupling and boundary coupling to the EK surface current are dependent upon Y_B, so that it is difficult to determine more accurately their relative importance in this role.

A comparison of the inhomogeneous sheath currents of Figs. 2 and 3 with the corresponding vacuum sheath currents of Figs. 4 and 5 reveals some similarity in the results, especially for $K_p^{(z)}$. The z component of current for the inhomogeneous sheath (Fig. 3) varies with azimuthal angle φ in a way very similar to the sheathless case of Fig. 5, though having a magnitude somewhere between the X = 0 and X = 5 case of the vacuum sheath currents. In the case of the φ component of current, the φ variation of the current for the two sheath models is somewhat different, though the inhomogeneous sheath current magnitudes again lie roughly between the vacuum sheath results for X = 0 and X = 5. These observations are substantially in agreement with results presented by Miller and Olte (1966b) for normal EK wave incidence on an inhomogeneous sheath, in that the inhomogeneous sheath currents for either the hard or soft boundary can be approximated quite well from the vacuum sheath model if the sheath thickness X is regarded as a parameter.

Figure 6, which shows the magnitude of $K_p^{(z)}$ for the inhomogeneous sheath model, with the same parameter values as for the previous graphs, but with the sheath thickness $X = 10D_\ell$, further illustrates this equivalence between the results of the vacuum sheath and inhomogeneous sheath currents. A comparison of Figs. 3 and 6 shows that the current magnitude for the hard boundary and the $10D_\ell$ inhomogeneous sheath fluctuates more with azimuthal angle φ and is larger toward the back of the cylinder, than that for the $5D_\ell$

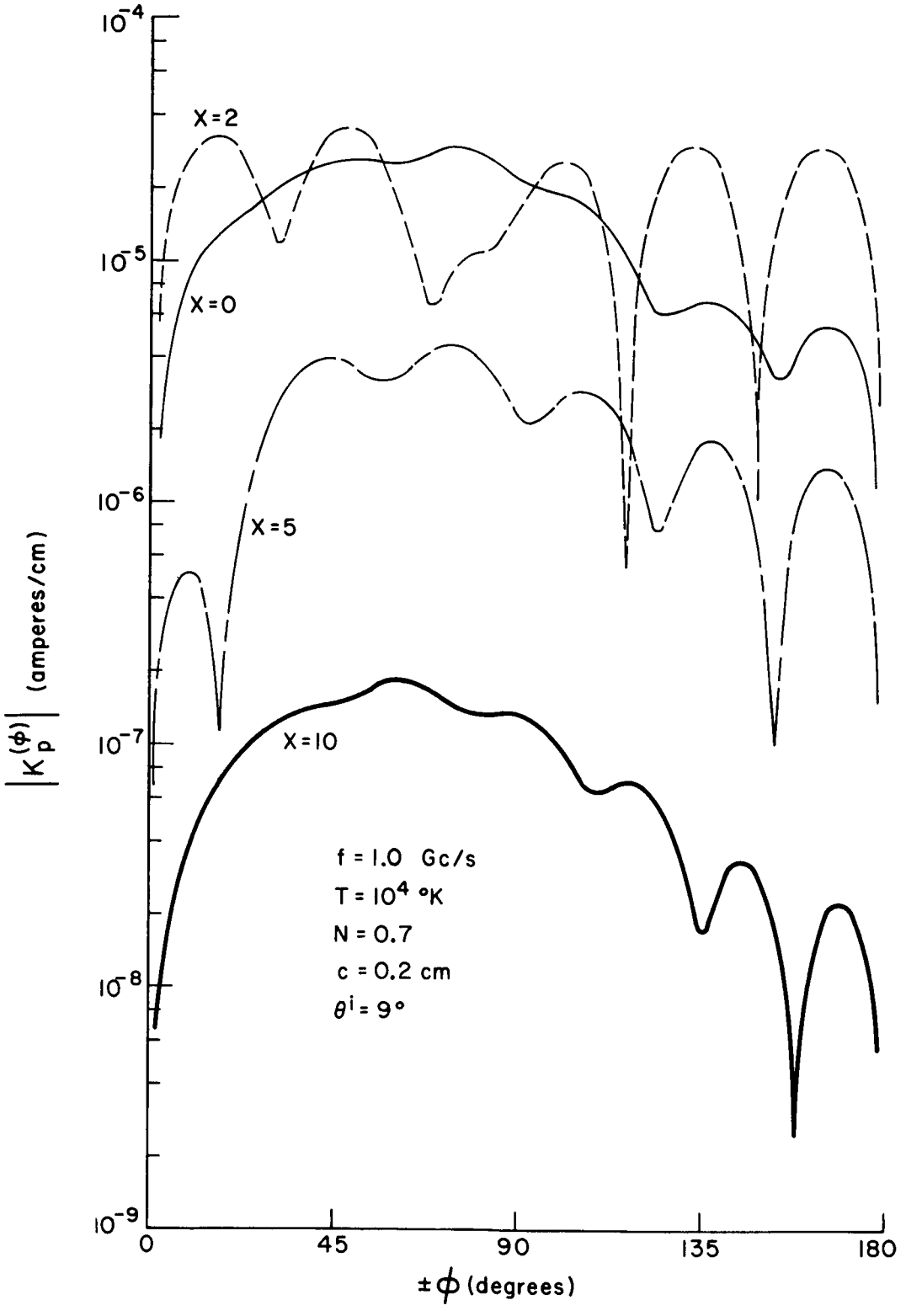

Fig. 4: The magnitude of $K_p^{(\varphi)}$ as a function of azimuthal angle φ for the vacuum sheath model with sheath thickness X a parameter and $\theta^i = 9^o$.

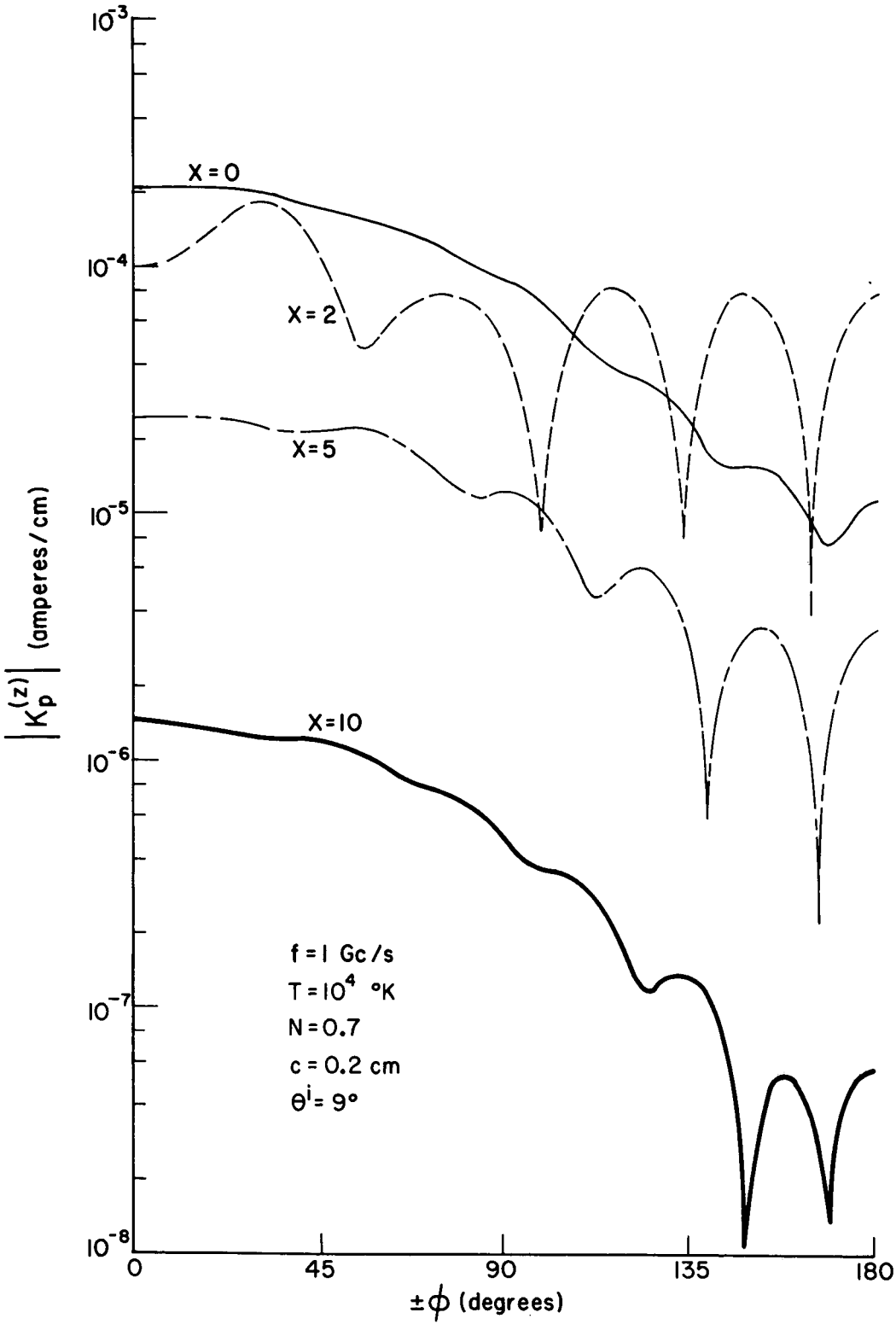

Fig. 5: The magnitude of $K_p^{(z)}$ as a function of azimuthal angle φ for the vacuum sheath model with sheath thickness X a parameter and $\theta^i = 9^o$.

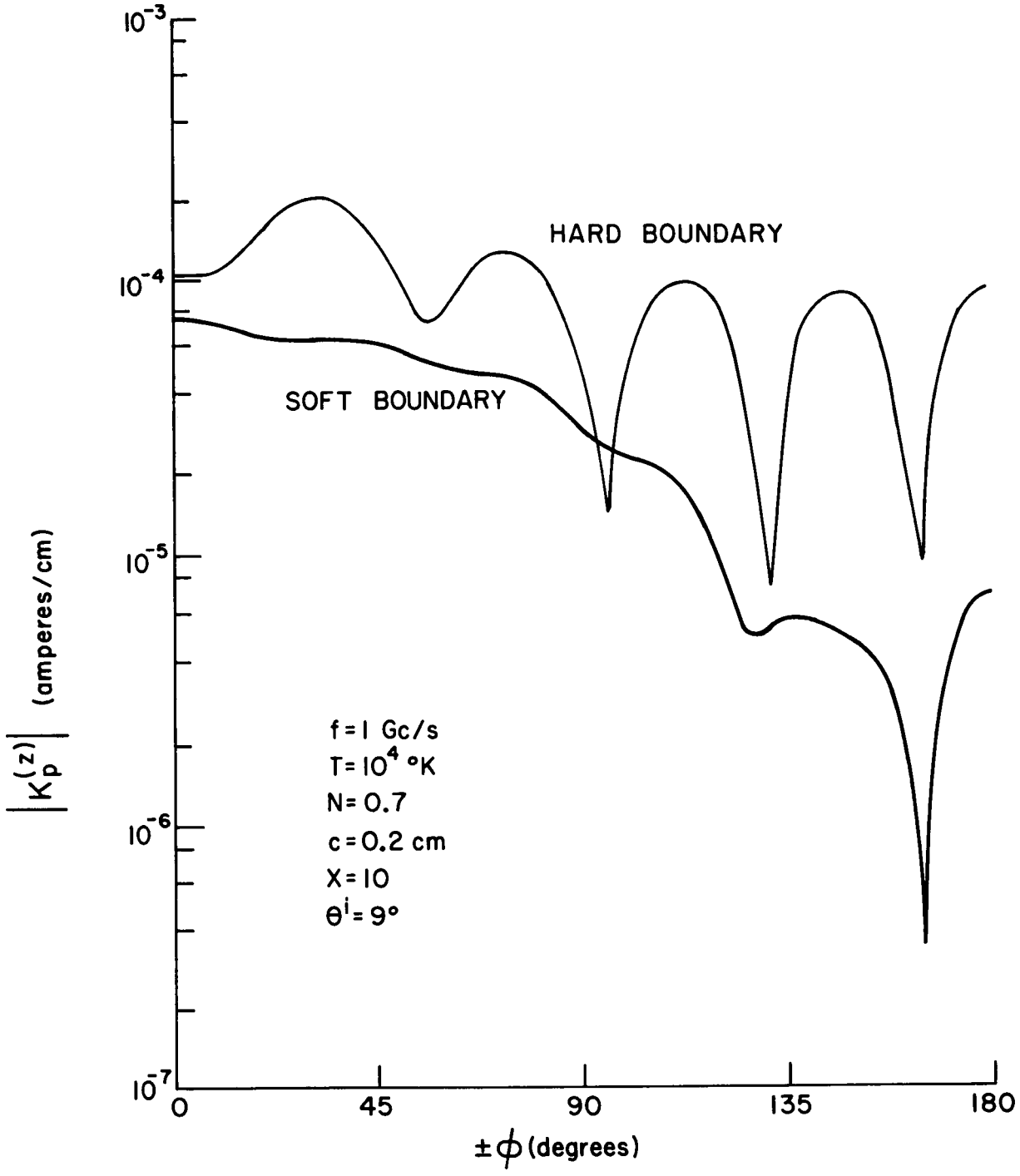

Fig. 6: The magnitude of $K_p^{(z)}$ as a function of azimuthal angle φ for the inhomogeneous sheath model with $X = 10$ and $\theta^i = 9^o$.

thick inhomogeneous sheath, while those for the soft boundary are quite similar. It may also be seen, in comparing Figs. 5 and 6, that the $2D_\ell$ thick vacuum sheath and $10D_\ell$ thick hard boundary, inhomogeneous sheath current magnitudes are very similar, as are the soft boundary inhomogeneous sheath and the $5D_\ell$ thick vacuum sheath currents of the same figures.

The final graphs of this series, Figs. 7 and 8, show the magnitude of $K_p^{(z)}$ only, from the inhomogeneous sheath model for a sheath $5D_\ell$ thick, and the vacuum sheath model for various sheath thicknesses, for an angle of incidence $\theta^i = 45^o$. We note in Fig. 7 that, as in the case of $K_p^{(\varphi)}$ for $\theta^i = 9^o$, the soft boundary current exceeds that for the hard boundary towards the back of the cylinder. Consequently, it appears that boundary and inhomogeneity coupling are of nearly the same importance. In comparing the inhomogeneous and vacuum sheath currents of Figs. 7 and 8 the inhomogeneous sheath currents are generally bracketed between the $X = 2$ and $X = 5$ currents for the vacuum sheath.

b. Incident EM Wave

Since the currents excited by the EM wave on a cylinder which is small in diameter compared with the wavelength vary in a regular way with azimuthal angle φ, the situation of interest here, we present only the maximum value of the current magnitude obtained from the φ variation as a function of angle of incidence, in Fig. 9. The TE and TM currents are denoted respectively by $K_e^{(\ )}$ and $K_m^{(\ )}$. Results from both a vacuum sheath of 0 and $10D_\ell$ thickness and an inhomogeneous sheath $20D_\ell$ thick are shown in Fig. 9 when the difference between them are large enough to resolve graphically. The other parameter values are the same as those in previous graphs. We see in Fig. 9 that only the TM wave produces currents which are appreciably affected by the presence of the sheath. It is interesting to observe that the vacuum sheath of $10D_\ell$ thickness appears to approximate the $20D_\ell$

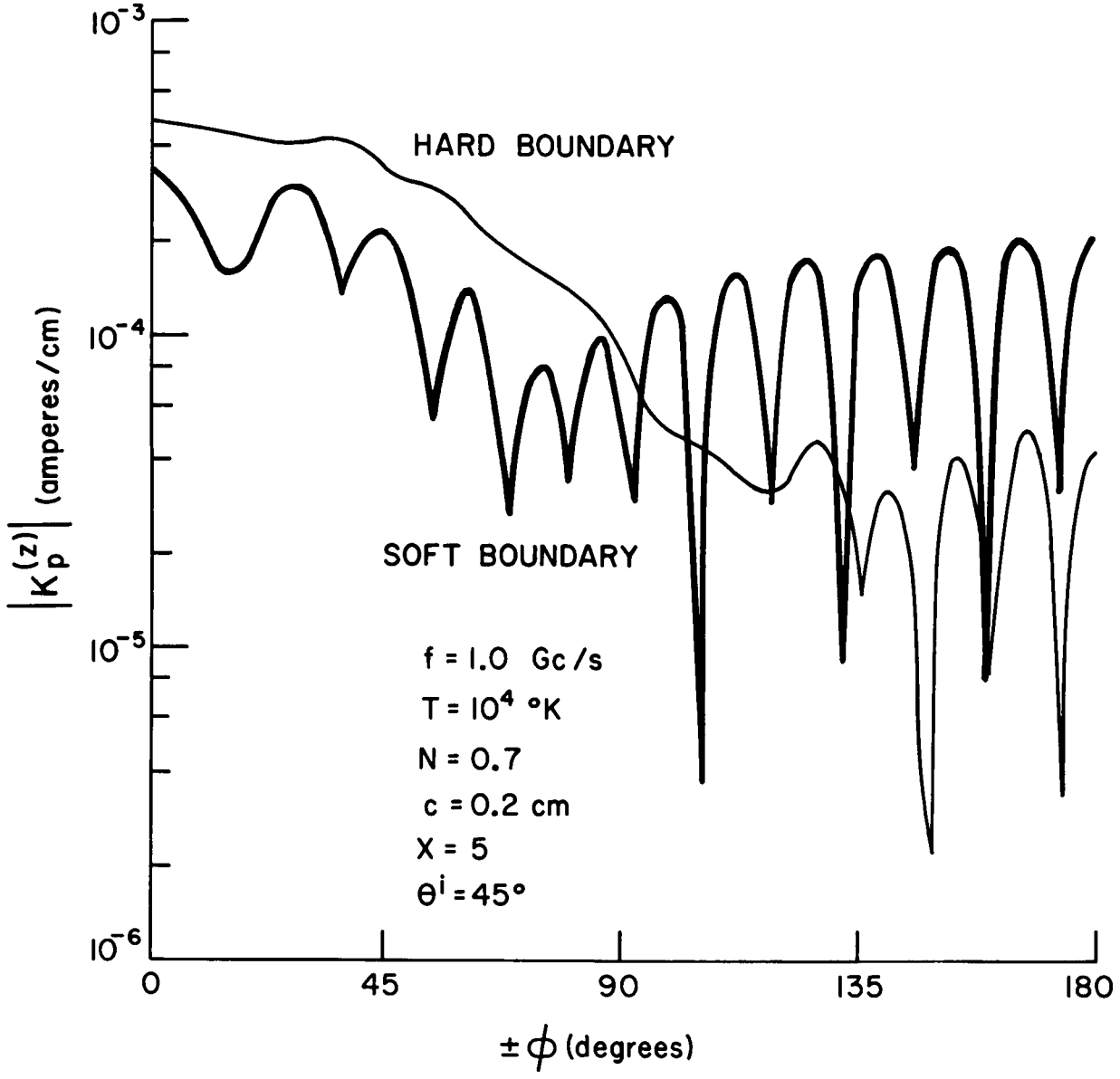

Fig. 7: The magnitude of $K_p^{(z)}$ as a function of azimuthal angle φ for the inhomogeneous sheath model with X = 5 and $\theta^i = 45^o$.

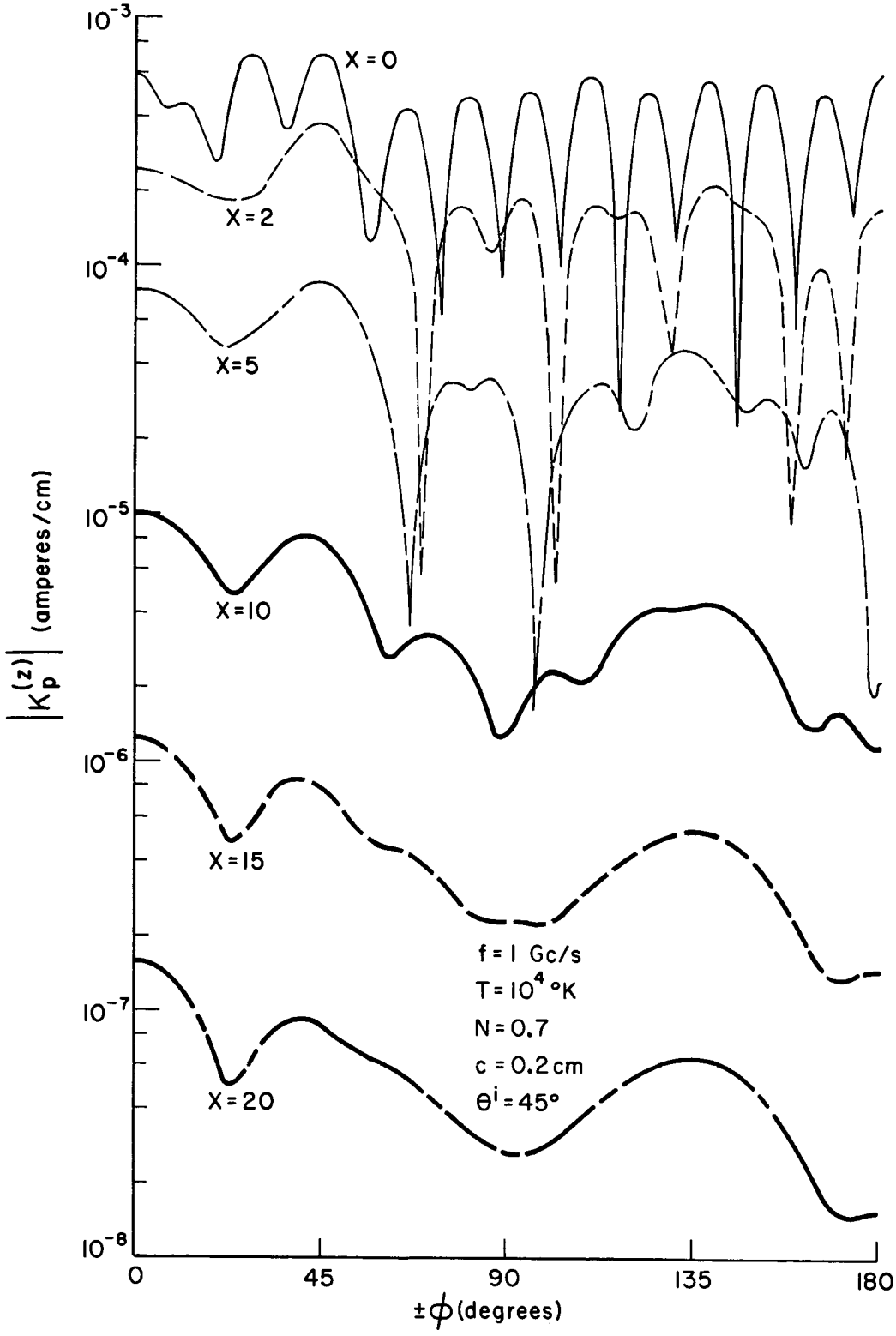

Fig. 8: The magnitude of $K_p^{(z)}$ as a function of azimuthal angle φ for the vacuum sheath model with sheath thickness X a parameter and $\theta^i = 45^o$.

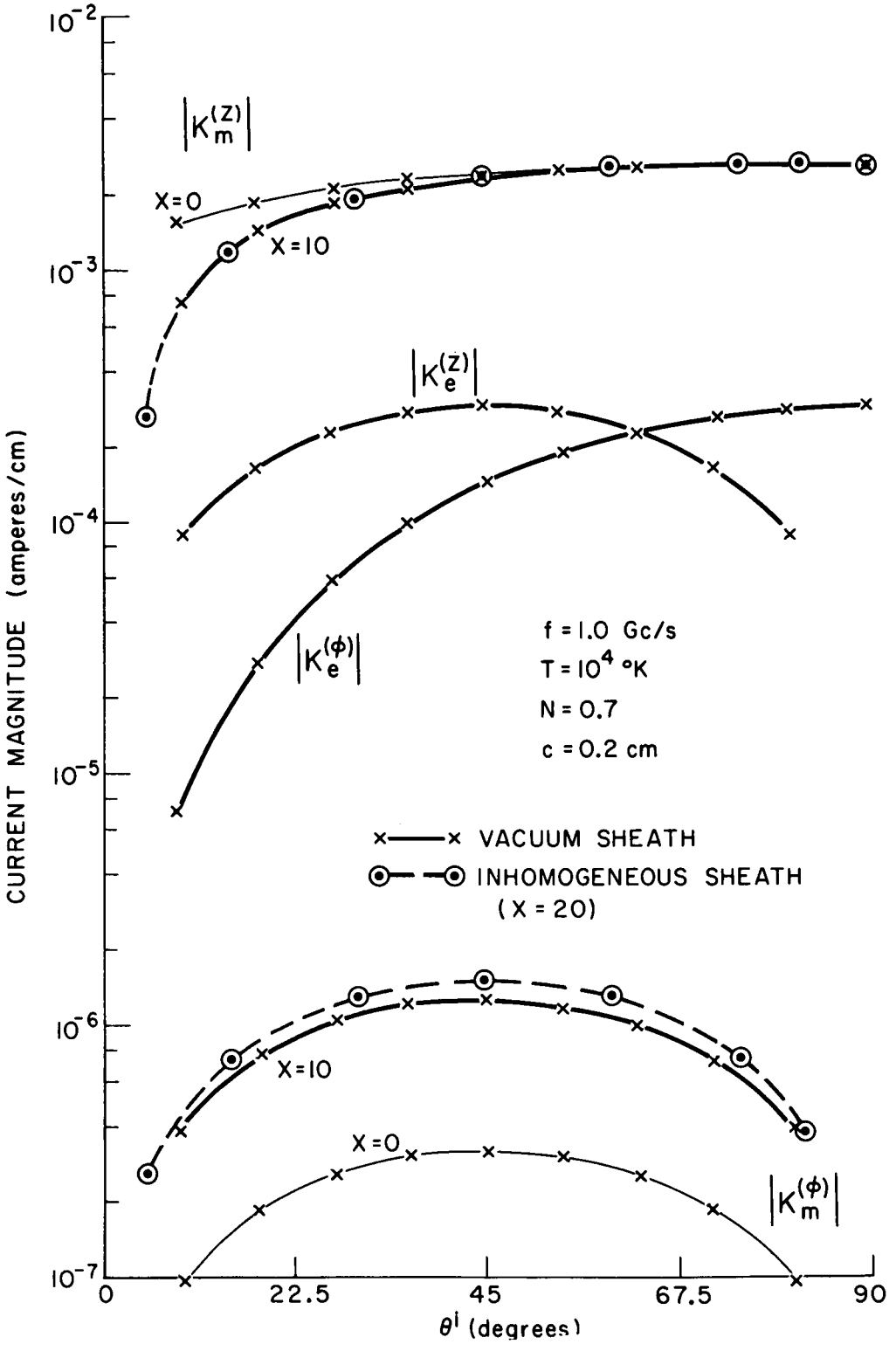

Fig. 9: The maximum current magnitudes for EM wave incidence as a function of angle of incidence θ^i for both the vacuum sheath (X = 0, 10) and the inhomogeneous sheath (X=20) models.

thick inhomogeneous sheath quite well, at least as far as the surface current produced by the TM wave is concerned. It should also be noted that the φ component of TM current, $K_m^{(\varphi)}$, is increased by the sheath, compared with the sheathless case. This occurs because while the TM wave excites no component of current on an infinitely conducting cylinder in free space, both the sheath vacuum and inhomogeneous and finite plasma temperature cause its excitation. Thus increasing the sheath thickness can result in an increase of $K_m^{(\varphi)}$.

Finally, it should be mentioned that the vacuum sheath calculations were performed for EM wave incidence, for the additional case of the cold plasma, i.e., T = 0, with changes on the order of 0.1 per cent or less occurring in the current magnitudes compared with the warm plasma results shown in Fig. 9, except for $K_m^{(\varphi)}$. For vacuum sheath thicknesses greater than about $2D_\ell$, $K_m^{(\varphi)}$ was similarly unaffected by setting T = 0, but as the vacuum sheath thickness was decreased towards zero, $K_m^{(\varphi)}$ became progressively smaller, becoming zero for X = 0 since then both of its excitation mechanisms are absent. We should note that for EM wave incidence, the cold plasma situation is the same as representing the vacuum sheath-uniform plasma interface as a soft boundary, since then the EM wave does not couple to an EK wave.

c. Comparison of EM and EK Currents

It should be recalled that the currents presented above are for the case of unit amplitude incident plane waves. One reasonable criterion for a comparison of the currents produced by the EM and EK waves would seem to be that when their power flow densities are equal. As discussed by Miller and Olte (1966a), the power flow density in the EK wave of potential

amplitude V_p^i equals that in an EM wave of potential amplitude V_e^i when

$$V_p^i = \frac{\omega_P}{\omega} \sqrt{\frac{v_r}{v_\ell}}\, V_e^i$$

where v_ℓ is the velocity of light in free space.

For the parameter values used here, this reduces to

$$V_p^i = 3.32 \times 10^{-2}\, V_e^i$$

If we use this equal power flow criterion, we see that the EK currents presented in Figs. 2-8 must be reduced by almost 2 orders of magnitude before they can be compared in amplitude with the EM currents of Fig. 9. The result is that only $K_m^{(\varphi)}$ of the EM currents is less than any of the EK currents, while the other EM current components are an order of magnitude or more larger than the EK currents. Consequently it appears that it would be difficult to measure the current produced by an EK wave in the presence of an EM background, an observation reached earlier by Miller and Olte (1966a) on the basis of the vacuum sheath analysis.

5. Comments and Conclusions

One of the most interesting aspects of the work reported here concerns a comparison of the inhomogeneous sheath and the vacuum sheath results. It was pointed out by Miller (1966) that linear increases in the vacuum sheath thickness beyond some minimum thickness on the order of $2D_\ell$, lead to exponential decreases in the surface current excited by the EK wave at oblique incidence on the infinite cylinder. This decrease in the current due to the EK wave is caused by the evanescent EM fields which it excites at the vacuum sheath-uniform plasma interface. One drawback of the vacuum sheath model is however, that the plasma in reality extends to the surface, with the result that any screening effect of the real sheath may be exaggerated by the vacuum sheath model.

As we have seen in the results presented above however, the vacuum sheath model can produce results for the surface currents for oblique EK wave incidence in good agreement with those of the inhomogeneous sheath models used, for a vacuum sheath thickness on the order of one-fifth to one-half the inhomogeneous sheath thickness. The equivalent vacuum sheath thickness is found to depend upon the cylinder surface admittance used in the inhomogeneous sheath calculations. For EM wave incidence, the equivalent vacuum sheath thickness appears to be about one-half the inhomogeneous sheath thickness. It thus appears that, despite its obvious physical shortcomings, the vacuum sheath model can serve a useful purpose in finding the surface currents excited by EM and EK waves on a plasma-immersed obstacle.

Perhaps the most significant finding of the inhomogeneous sheath results for EK wave incidence, is the relatively small dependence of the current on the surface admittance of the cylinder, showing that the boundary coupling and inhomogeneity coupling mechanisms are of nearly the same importance in converting the incident EK wave to a scattered EM wave. This is important since the hard boundary is an admitted oversimplification for representing the interaction of the electrons moving under the influence of the wave electric fields in the plasma with the cylinder surface. The effect of the sheath and coupling to the EK wave has been found to have a small influence on the surface currents excited by the EM wave. An area for further investigation would be comparison of the scattering cross-section of plasma-immersed obstacles for the vacuum sheath and inhomogeneous sheath models, especially for an incident EM wave.

REFERENCES

Cohen, M. (1962), Radiation in a Plasma III: Metal Boundaries, Phys. Rev. 126, 398-404

Miller, E. K. (1966), Surface Current Excitation by Electromagnetic and Electrokinetic Waves on a Plasma Immersed Cylinder; to be published as a High Altitude Engineering Laboratory Report, University of Michigan, Ann Arbor, Michigan.

Miller, E. K. and A. Olte (1966a), Excitation of Surface Currents on a Plasma-Immersed Cylinder by Electromagnetic and Electrokinetic Waves I. The Vacuum Sheath; to be published in Radio Science.

Miller, E. K. and A. Olte (1966b), Excitation of Surface Currents on a Plamsa-Immersed Cylinder by Electromagnetic and Electrokinetic Waves II. The inhomogeneous Sheath; to be published in Radio Science.

Ralston, A. (1965), A first Course in Numerical Analysis, McGraw-Hill Book Co.

Self, S. A (1963), Exact Solution of the collisionless Plasma Sheath Equation, Phys. Fluids 6, No. 12, 1762-1768.